



## LESSONS LEARNED

# Solidification Cracking of Longitudinal Submerged Arc Welded Pipes

Rajesh K. Goyal · Ankit Singh · T. S. Kathayat

Submitted: 9 March 2020 / Published online: 28 May 2020  
© ASM International 2020

**Abstract** High-strength longitudinal submerged arc welded (LSAW) pipes are used by the oil and gas operators for long-distance fluid transfer. During manufacturing of 18-m-long LSAW pipes, numerous T-end (Tail end) cracks were observed by manual ultrasonic testing. A failure investigation was carried out on weld crack formed approximately 40–150 mm away from T-end of a 762 mm OD × 15.8 mm WT × 18,000-mm-long API 5L X70M grade pipes. The present paper discusses the analysis of end cracks with the help of NDT, microhardness, metallography, SEM and EDS analyses and possible factors responsible for the T-end cracks. The high strength of parent material, a longer length of the weld seam and transverse displacement were observed as the possible causes for the formation of solidification cracks at one end of LSAW pipes.

**Keywords** JCO-E · LSAW · TRB · Transverse displacements · Microfissures · T-end

## Introduction

The welding, an integral process in the pipe manufacturing industry, has a direct influence on thermal and mechanical properties and the integrity of the product during service. Due to the high temperatures introduced during welding and the subsequent cooling of the welded metal, welding can produce undesirable residual stresses and deformations [1]. The forming of a pipe is cold work giving shape to thermo-mechanical controlled processing (TMCP) plate

into a pipe at various stages. Longitudinal submerged arc welded (LSAW) pipes are manufactured by JCO-E process. In J-C-O, the formation of the pipe is carried out by incremental pressing with the required number of strokes to form the high-strength pipe with less forming force. The spring back behaviour of high-strength steel pipe can be controlled up to a certain extent by controlling the depth of each stroke during the J-C-O formation [2]. The formation of pipe from the TMCP plate mainly consists of edge milling to the required width and weld joint geometry. The milled plate is then formed by bending to the required radius along the length of the plate, and it is known as ‘edge crimping’. The edge crimped plate is then formed to pipe shape through J-C-O process by making first ‘J-shape’ then ‘C-shape’ and finally O-shape as shown in Fig. 1. Continuous gas metal arc weld (GMAW) tack welding is performed on formed pipes from outside, and further submerged arc welding (SAW) is done from inside and outside. After long seam welding, the welded pipe is mechanically expanded from inside to achieve the final dimensions and to relieve the residual stresses present in the formed pipe. A failure investigation was carried out for longitudinal weld centreline crack which formed at the one end of the weld after mechanical expansion, for the pipes having dimensions of 762 mm OD × 15.8 mm WT × 18,000 mm length of APL 5L X70M grade. The failure mechanism was identified, highlighting factors that contributed to the welded pipe failure. Finally, recommendations were proposed to avoid this type of pipe failure.

---

R. K. Goyal (✉) · A. Singh · T. S. Kathayat  
Welspun Corp Ltd, Anjar 370110, India  
e-mail: goyal\_rajesh@welspun.com

**Fig. 1** Schematic diagram of JCO-E pipe forming process

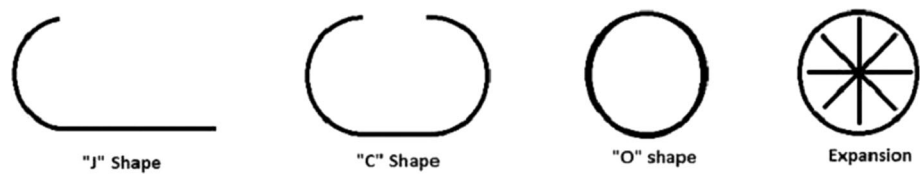


**Table 1** GMAW tack weld parameters

DC (A)	DC (V)	Speed (m/min)	CO <sub>2</sub> flow rate (LPM)	Heat input (kJ/mm)
GMAW tack weld				
1055	24	5	60	30

**Table 2** Inside (ID) and outside (OD) SAW weld parameter

Parameter	DC (A)	AC1 (A)	AC2 (A)	DC (V)	AC1 (V)	AC2 (V)	Speed (m/min)	Heat input (kJ/mm)
ID side SAW	750	700	600	34	36	39	1.6	2.78
OD side SAW	975	825	600	34	36	39	1.68	3.12

## Methodology

GMAW continuous tack welding was performed with 3.2 mm ER70S-6 wire. Inside (ID) and outside (OD) SAW single-pass welding was carried out with EM12K + EA2TiB type 3 wires (DC + AC1 + AC2) and 995 N flux. The GMAW and SAW welding parameter are shown in Tables 1 and 2, respectively.

Various corrective actions were taken at edge milling, forming, tack welding and ID welding during the pipe manufacturing process to overcome the crack at T-end of the pipe. The T-end was reversed during expansion, but again, the indications were found at the same welding finish end and in the same proportion. The run-in and run-out tabs welded were reassured for their weld length on the tabs, and no appreciable change was noticed. The % of expansion was reduced from 1.25 to 1.1%; however, no appreciable change in % of flaw detection and location was observed.

Specimens were cut from the end of the pipe for visual and NDT inspection to examine the flaw. Chemical analysis of the weld section was carried out with optical emission spectroscopy. Samples were fine polished and etched with 3% nital for metallographic investigation employing optical microscopy and scanning electron microscopy equipped with an energy dispersive spectrometer (EDS). Microhardness testing was carried out around the vicinity of cracks.

## Results and Discussions

### Visual and Non-destructive Test (NDT) Inspection

Visual inspection on inside and outside surface of weld showed smooth surface and presence of weld bead at the

centre. Visually, no defects were observed. During real-time radiography (RTR) and x-ray test, no indication of the flaw was observed. Manual ultrasonic test (MUT) was performed at both ends of the pipe to inspect the weld seam that revealed the indications of flaw having 79–350 μm height, 8.5 μm width at the tail end, within around 160 mm length from the end as shown in Fig. 2.

Magnetic particle inspection (MPI) test on samples' weld bead surface and the transverse cut section was unable to detect any significant flaw as shown in Fig. 3.

### Chemical Analysis

The results of chemical analyses at inside weld, outside weld and base metal location show that the pipe material meets the chemical composition requirement of API 5L X70M as shown in Table 3. The chemical composition of weld metal appears to match with the parent material. The weld cracking tendency factor is given as:

$$230(\%C) + 190(\%S) + 75(\%P) + 45(\%Nb) - 12.3(\%Si) - 5.4(\%Mn) - 1 \quad (\text{Eq 1})$$

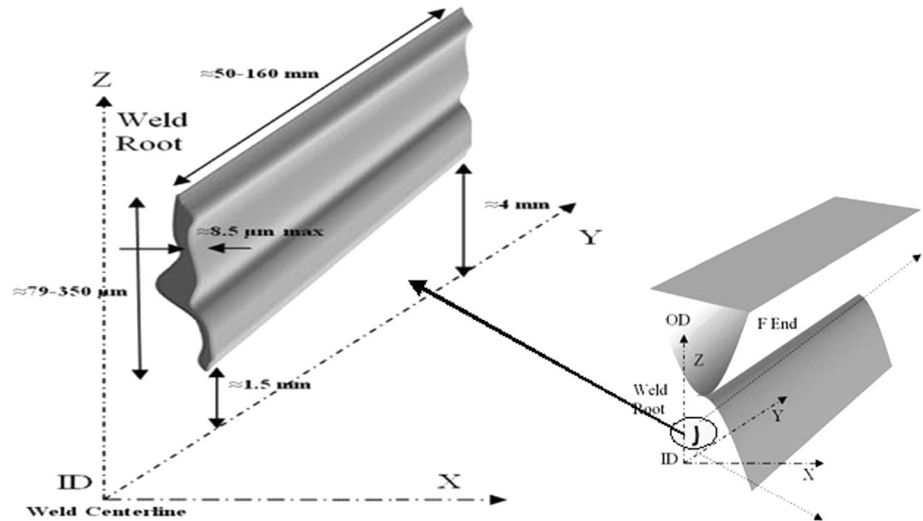
which is less than 30; hence the composition is normal.

### Metallographic Analysis

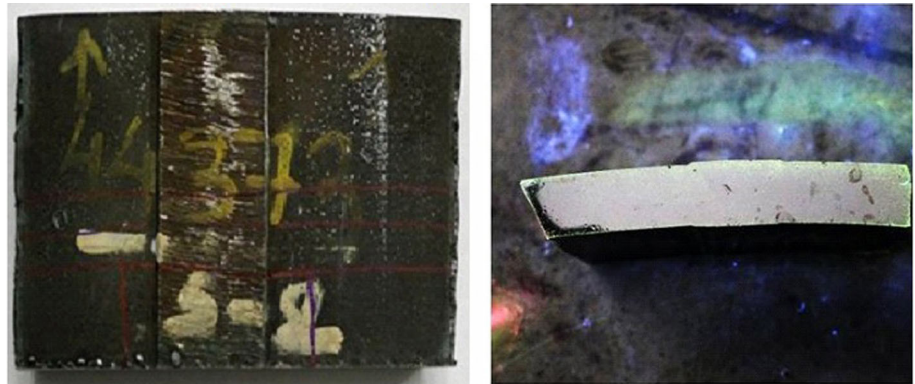
#### Macro- and Microstructure Analysis

The macro-structural examination across the transverse section showed sound weld quality along with proper fusion. The width-to-depth ratio of the weld (w/d) appears to be normal. Though, the microstructure revealed a crack at the inside weld centreline. Crack was propagating in the transgranular and intergranular manner in some locations as shown in Fig. 4.

**Fig. 2** Schematic diagram of flaw detected by MUT



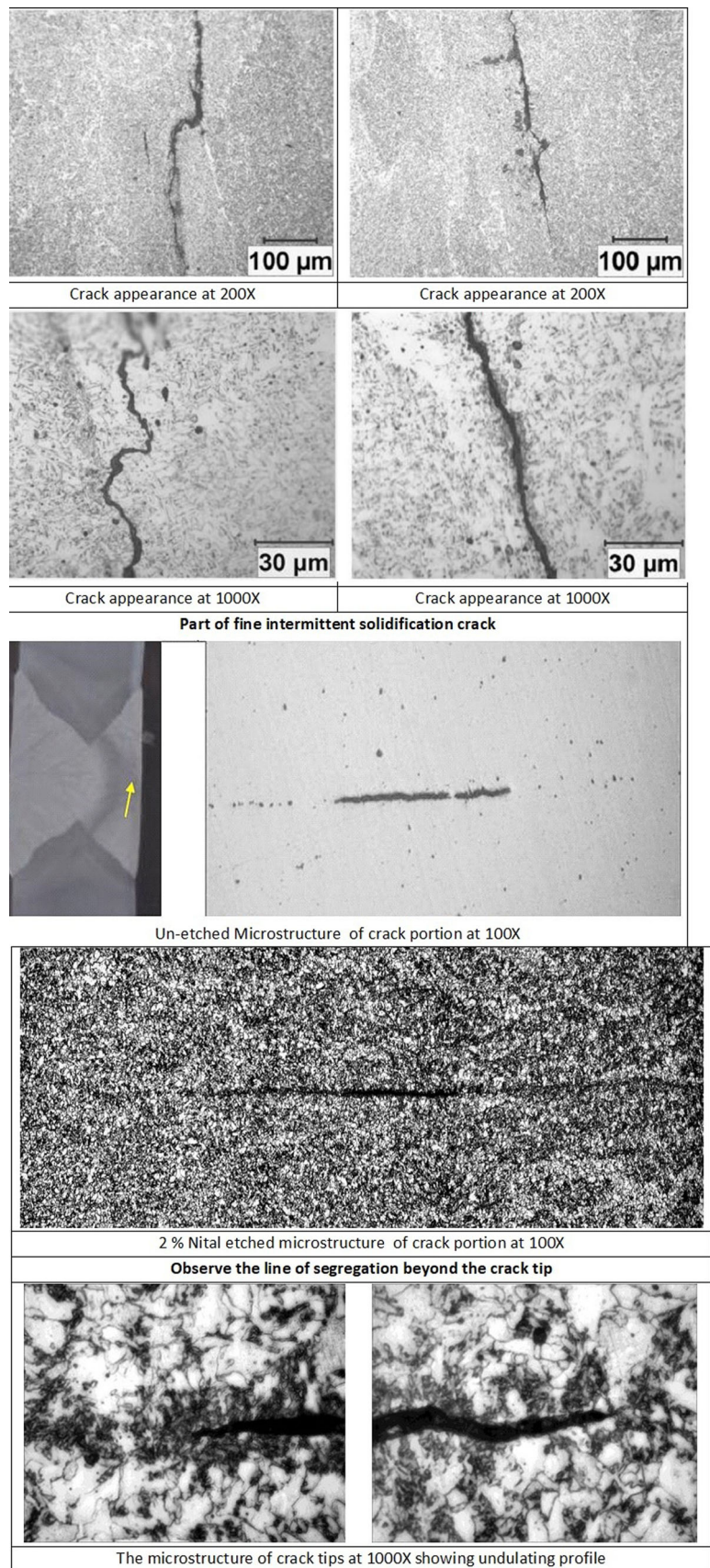
**Fig. 3** Magnetic particle inspection (MPI) on flaw detected portion. (a) Test coupon on which defect was located for further analysis. (b) MPI on transverse cross section



**Table 3** Chemical analysis results for base metal (BM), outside weld and inside weld location

Elements	C	S	P	Mn	Si	Al	Ti	Nb	Cr	CE <sub>(Pcm)</sub>	CE <sub>IW</sub>
BM	0.04	0.001	0.01	1.55	0.35	0.035	0.02	0.05	0.15	0.14	0.34
OD weld	0.035	0.0057	0.018	1.67	0.419	0.017	0.025	0.02	0.122	0.152	0.375
ID weld	0.035	0.0057	0.019	1.72	0.408	0.016	0.017	0.022	0.131	0.15	0.373

**Fig. 4** Microstructures obtained at crack vicinity





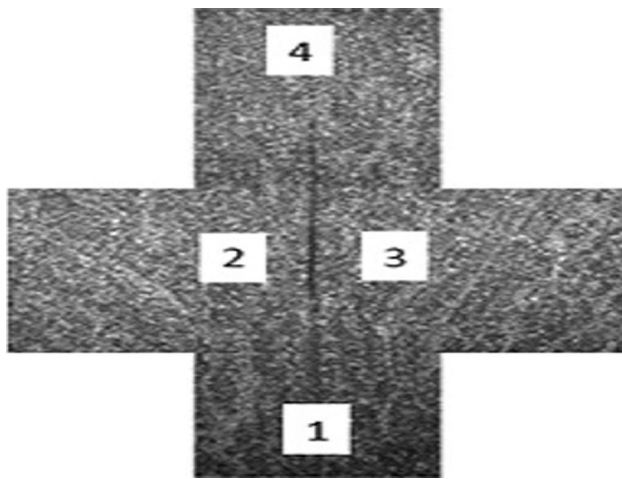


**Fig. 5** Microhardness measurement profile

### Hardness Testing

Microhardness measurement was carried out with 100 gf load around the crack areas which shows higher hardness  $\sim 262$  Hv10 at crack tips locations 1 and 4 and moderate hardness on both sides of crack  $\sim 210$  Hv10 at locations 2 and 3 (Fig. 5).

### SEM and EDS Analysis

The results of scanning electron microscopy (SEM) with energy-dispersive spectrometer (EDS) maps around crack vicinity are shown in Fig. 6. EDS analysis at crack tip shows the presence of oxygen, aluminium, sulphur, manganese and iron which are an indication of the presence of inclusions in the analysed sample.

Microcracks in longitudinal direction were observed at one end of the pipe into the inside weld. The visual examination could not reveal any surface flaw, with unaided eye observation. Weld bead quality appears to be normal on both sides.

Random samples were sectioned from the T-end of the pipe before expansion and examined under the optical microscope. Microexamination reveals microfissures at the T-end, but these were not reported by MUT, x-ray and MPI because of having microsize. The cracks were observed

after the mechanical expansion during MUT. MPI test carried out on the transverse cross section of the weld, with the known position of crack could not reveal the presence of the flaw. The flaw does not get revealed by other NDT methods like RTR and x-ray. The defects are formed at approximately 40–150 mm away from T-end of the pipe. The chemical composition results show that the pipe material meets the chemical composition requirement of API 5L X70M PSL2 grade.

The chemical composition of weld metal appears to be compatible with the pipe parent material. The weld pool contains titanium and niobium as microalloying elements. The microstructural examination across the transverse section shows sound weld quality with proper fusion and width-to-depth ratio. Hardness at crack tip was 40–50 Hv10 higher compared to weld. SEM shows a longitudinal crack in the weld. Its opening is quite uneven with fine tips. The crack features are that of mechanical tearing with both inter and transgranular mode of propagation. EDS analysis at crack tip shows the presence of oxygen, aluminium, sulphur and manganese which is indicative of the presence of inclusions (Table 4).

### Discussions

Most of the microfissures have occurred in heats of plates having more than 530 MPa yield strength (YS). No such cracking was taking place on previous lots of raw material that were having YS at lower side supplied by another steel supplier. SEM and EDS analysis showed the presence of inclusion forming elements at its vicinities like Manganese, Sulphur, Oxygen and Aluminium.

The solidification cracks were found to be interdendritic and intergranular with respect to the solidifying grains. Also, the presence of a line of segregation beyond the crack tip (with undulating profile) confirms that the cracking resulted from the presence of manganese, oxygen, aluminium and sulphur in the flux material.

Since there was no liquation crack present in the HAZ, so nothing can be said about the actual initiator of the solidification crack.

**Fig. 6** SEM-EDS analysis around crack vicinity

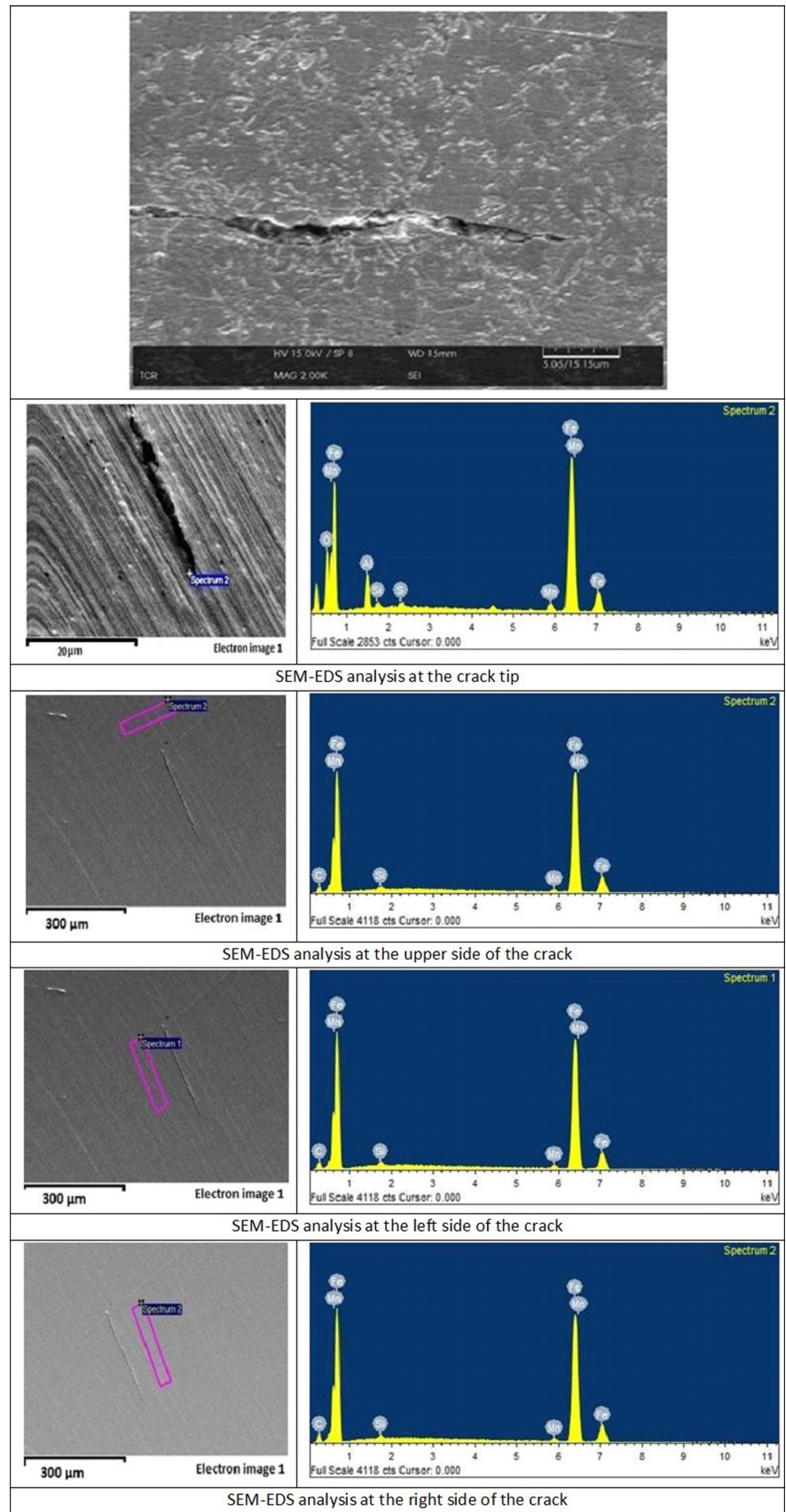


**Table 4** EDS analysis results for crack

Elements	Wt.% inside the crack	Wt.% surrounding the crack
Oxygen	3.66	
Aluminium	4.22	
Silicon	0.59	0.47
Sulphur	0.52	
Manganese	3.46	1.75
Iron	87.54	96.32

## Conclusions

The microfissures seen at the end of the weld are typically solidification cracks which may be due to the presence of elements such as manganese, oxygen, aluminium and sulphur. This crack further expanded on the mechanical expansion of the pipe. The strain might be accumulated due to below-mentioned reasons:

- Pipes ends were having higher spring back effect that aids in creating the microstrains during solidification.
- Higher strength of the base metal contributes to higher residual stresses.

- The residual stresses were higher at the tail end of the weld where the weld finishes.
- Due to accumulated strain, additional strain appeared during mechanical expansion.

To overcome such problem in the project, nickel wire was used which raises the overall temperature of the weld pool allowing greater duration for solidification to take place and hence, lesser residual stress shall be generated in the weld metal.

**Acknowledgments** Authors are thankful to the management of Welspun Corp Ltd for giving support and permission to prepare and publish this paper.

## References

1. A. Yaghi and A.A. Becker. State of the Art Review-Weld Simulation Using Finite Element Methods Report FENET-UNOTT-DLE-08
2. J. DevChandel, N. Singh, formation of X-120 M line pipe through J-C-O-E technique. *Sci. Res. Eng.* **3**, 400–410 (2011)

**Publisher's Note** Springer Nature remains neutral with regard to jurisdictional claims in published maps and institutional affiliations.